Harmonic generation by the H_2^+ molecular ion in intense laser fields

T. Zuo, S. Chelkowski, and A. D. Bandrauk

Laboratoire de Chimie Théorique, Faculté des Sciences, Université de Sherbrooke, Sherbrooke, Québec, Canada J1K 2R1

The harmonic-generation (HG) spectra of the H_2^+ molecular ion generated by short, intense, linearly polarized laser pulses are calculated nonperturbatively by solving a three-dimensional time-dependent Schrödinger equation. It is found that while H_2^+ radiates in a similar manner to an atomic system such as H or He^+ at high frequencies, the molecular ion in high-vibrational states or at large internuclear distances behaves analogously to a two-level system in an intense, relatively-long-wavelength laser field. It will be shown that symmetric molecular ions should in general produce more efficient harmonic generation than atoms, due to the presence of molecular charge-resonance (CR) states, which have no atomic analogues. Two HG plateaus, one molecular due to CR transitions and one atomiclike, appear for a long-wavelength excitation. Each plateau has its own maximum harmonic-number cutoff, which can be rationalized in terms of the maximum energy which can be acquired by an electron in the laser field.

I. INTRODUCTION

It is well known that when a quantum system is subject to an intense laser field, the response of the system to the external field becomes highly nonlinear as the laser intensity rises to the order of 10^{13} W/cm^2 and higher. One of the consequences of this nonlinear response is the radiation of photons by the system at frequencies of multiples of the laser fundamental frequency, normally called harmonic generation (HG). HG of atomic systems in intense laser fields has been an area of very active research over the last several years both theoretically and experimentally (see, e.g., the review [1]).

Research in the harmonic generation for molecular systems is, however, at its early stage. Krause, Schafer, and Kulander [2] did a calculation for the harmonic generation of the H_2 molecule which is stretched to have the same ionization potential as the H atom. Similar HG spectra were obtained compared with that of the H atom. Recently Ivanov, Corkum, and Dietrich [3] proposed a way to coherently control the HG for a strongly-laser-driven two-level analytic model with application to molecular ions in mind. In this work we investigate numerically the harmonic generation by the H_2^+ molecular ion in an intense, linearly polarized laser field. The laser intensity varies from 10^{13} W/cm^2 to over 10^{14} W/cm^2. Several wavelengths (228 nm, 1064 nm and 1380 nm) have been scanned. We focus on the comparison between the HG spectra of H_2^+ and those of the H atom and the He^+ ion. One of the common and well known features of HG spectra in atomic systems is the existence of the so-called "plateau" which exhibits a relatively broad range of high harmonic peaks of roughly the same strength, followed by a sharp cutoff. This is an important manifestation of the nonperturbative nature of the harmonic generation. We are particularly interested in testing the validity of a quasiempirical and rather successful formula proposed by Krause, Schafer, and Kulander [4] and Corkum

[5] to estimate the length and cutoff of the plateau for the molecular system.

Molecular ions such as H_2^+ have pairs of electronic states known as the charge-resonance (CR) states. These CR states are very strongly coupled to electromagnetic fields for large internuclear distance R since in fact, the dipole moment between the CR states becomes $R/2$ asymptotically [6], see also Fig. 1. Bandrauk and co-workers first pointed out the importance of these charge-resonance electronic states as sources of highly nonlinear laser-induced effects in molecules [7]. Thus laser-induced avoided crossings [7,8], above threshold photodissociation [9,10], and molecular stabilization [11,12] are highly nonlinear laser-induced photophysical phenomena which have been predicted to occur based on the dressed state molecule representation of the CR states. These laser-induced nonlinear phenomena have now been observed experimentally [13–15]. Ivanov and Corkum [16] have re-
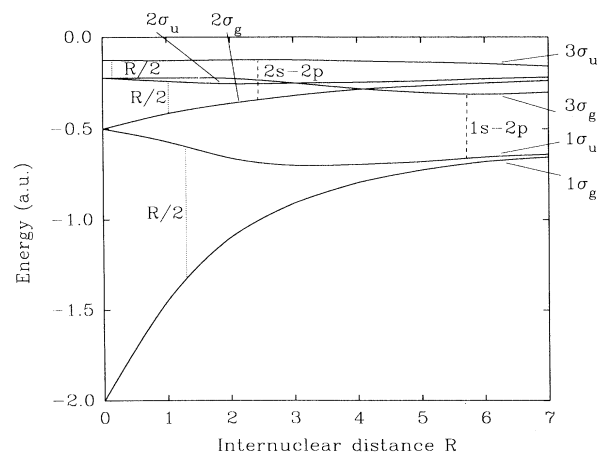

FIG. 1. Energy levels of some lowest states of H_2^+.

cently examined the possibility of using the CR states of molecular ions to produce and coherently control HG. Their calculations were based on an analytic two-level model as a limiting case due to the strong radiative coupling of the CR states and the isolation of these CR states from other molecular levels at large R. In this work, we carry out full calculations in this regime for the H_2^+ molecule ion aiming at a confirmation of the two-level theory and in particular to examine the influence of other upper energy levels and ionization on HG that were ignored in the two-level theory. The results are also compared to the separated atom limit ($R = \infty$) which is H and the united atom limit ($R = 0$) which is He^+ (Fig. 1).

II. TWO-LEVEL MODEL AND CR STATES

Figure 1 shows some of the lowest electronic levels of the H_2^+ molecular ion [17]. We have indicated some of the atomic transitions which remain in the molecular case, e.g., $1s \rightarrow 2p$, $2s \rightarrow 2p$, etc. Of note is that $ns \rightarrow np$, transitions which are degenerate in the atom, are no longer degenerate in the molecule. As we will show below, degenerate transitions cannot generate harmonics, i.e., only nondegenerate transitions are the source of harmonic generation. Most important, however, is the fact that transitions between molecular orbitals of different symmetry but which are degenerate at the separated atom limit ($R = \infty$ or H), e.g., $n\sigma_g \rightarrow n\sigma_u$, have electronic transition moments which diverge as $R/2$ [6,7], due to resonance charge exchange between degenerate atomic orbitals. These were shown first by Bandrauk and co-workers to give rise to highly nonlinear effects in photodissociation [7–12]. One sees clearly from Fig. 1 that at large distances the lowest CR transition, $1\sigma_g \rightarrow 1\sigma_u$, separates in energy from other higher-energy CR transitions and can thus be treated as an isolated two-level system. We summarize by pointing out that in H_2^+ new transitions occur as a source of HG: (a) degenerate atomic transitions become nondegenerate; (b) CR transitions with diverging transition moments should dominate at large R.

Based on analytic solutions of the time-dependent Schrödinger equation from a two-level system with Rabi frequency Ω_R much larger than the energy separation ω_0, Ivanov and Corkum have predicted that such CR transitions should be the source of very efficient harmonic generations [3,16]. We reexamine in this section the harmonic generation produced by a strongly driven two-level system using optical Bloch equations [18]. This allows us to establish the value of the harmonic cutoff or equivalently the maximum number of the harmonics generated. The wave function of a two-level system can be taken to be

$$|\psi(t)\rangle = a_1(t)|\psi_1\rangle + a_2(t)|\psi_2\rangle. \qquad (1)$$

The corresponding time-dependent Schrödinger equation takes on the form

$$i\dot{a_1} = -(\omega_0/2)a_1 + V(t)a_2, \qquad (2a)$$

$$i\dot{a_2} = (\omega_0/2)a_2 + V(t)a_1, \qquad (2b)$$

where $\omega_0 = (E_1 - E_2)/\hbar$ is the transition frequency, $V(t) = -p_{1,2}E(t)/\hbar$, $p_{1,2}$ is the transition dipole moment, and $E(t)$ is the external field. Often, it is more convenient to use Bloch equations, which are three real differential equations instead of two complex ones. One defines three real functions [18],

$$x(t) = a_1 a_2^* + a_2 a_1^*, \qquad (3a)$$

$$y(t) = i(a_2 a_1^* - a_1 a_2^*), \qquad (3b)$$

$$z(t) = |a_1|^2 - |a_2|^2. \qquad (3c)$$

$d(t) = p_{1,2}x(t)$ is the induced dipole moment and $z(t)$ is the population inversion. One derives easily the corresponding Bloch equation by differentiating (3) and using (2). One then gets

$$\dot{x} = -\omega_0 y, \qquad (4a)$$

$$\dot{y} = \omega_0 x + 2V(t)z, \qquad (4b)$$

$$\dot{z} = -2V(t)y. \qquad (4c)$$

These equations have the constant of motion $x^2 + y^2 + z^2$ which is set to one (the normalization of the wave function). Equations (4b) and (4c) can be easily solved in the strong field regime, when $|V(t)| \gg \omega_0$. Then, by neglecting ω_0 in (4b) one obtains the following strong field solutions:

$$y(t) = y(0)\cos[F(t)] + z(0)\sin[F(t)], \qquad (5a)$$

$$z(t) = z(0)\cos[F(t)] - y(0)\sin[F(t)], \qquad (5b)$$

$$F(t) = \int_0^t 2V(t')dt'. \qquad (5c)$$

For a monochromatic field $E(t) = E_M\cos(\omega t)$ one gets $F = 2\Omega_R/\omega \sin(\omega t)$ and

$$\dot{x} = -\omega_0\{y(0)\cos[\delta\sin(\omega t)] + z(0)\sin[\delta\sin(\omega t)]\}, \qquad (6)$$

where $\delta = 2\Omega_R/\omega$ is the coupling parameter and the Rabi frequency is defined as

$$\Omega_R = p_{1,2}E_M/\hbar. \qquad (7a)$$

A useful conversion formula for the Rabi frequency is

$$\Omega_R(\text{eV}) = 1.45 \times 10^{-7}[I \text{ (W/cm}^2)]^{1/2}[p \text{ (a.u.)}]. \qquad (7b)$$

The two trigonometric functions present in (6) have the following Fourier expansions [19]:

$$\cos[\delta\sin(\omega t)] = J_0(\delta) + 2\sum_{k=0}^{\infty} J_{2k}(\delta)\cos(2k\omega t), \qquad (8a)$$

$$\sin[\delta\sin(\omega t)] = 2\sum_{k=0}^{\infty} J_{2k+1}(\delta)\sin[(2k+1)\omega t]. \qquad (8b)$$

The first term, (8a), leads to the appearance of *even* harmonics while the second one yields the odd harmonics. By selecting initial conditions one can inhibit either one or the other, e.g., the choice

$$y(0) = 0 \text{ and } z(0) = \pm 1 \qquad (9)$$

gives only odd harmonics. In fact, it can be shown that the initial conditions depend strongly on the turn on of the pulse. Furthermore, it is easy to show that the choice (9) leading to pure odd-harmonic spectra corresponds to the case of a very slow, adiabatic turn on of the pulse [20]. Integrating (6) with the help of (8b) and (9) gives the induced dipole moment,

$$d(t) = p_{1,2}x(t)$$
$$= \frac{\pm 2p_{12}\omega_0}{\omega}\left[\sum_{k=0}^{\infty} J_{2k+1}(\delta)\cos[(2k+1)\omega t]/(2k+1)\right]. \qquad (10)$$

Thus the intensity I_N of the Nth- ($N = 2k+1$) order harmonic is proportional to

$$p_{1,2}^2\left(\frac{\omega_0 J_N(2\Omega_R/\omega)}{N\omega}\right)^2. \qquad (11)$$

Since the Bessel functions start to decrease quickly for their indexes greater than arguments the frequency cutoff or maximum harmonic N_m can be obtained from the asymptotic properties of Bessel functions [19],

$$N_m = 2\Omega_R/\omega. \qquad (12)$$

In fact the Bessel function $J_n(x)$ decreases monotonically but with different speed, e.g., for $x \approx n$ the behavior is proportional to $n^{-1/3}$ while for $n \gg x$ the behavior is $(x/2)^n/n!$. The maximum harmonic order according to Eq. (12) is defined by this last asymptotic behavior. We note that since $\Omega_R = eRE_M/2$, $2\Omega_R = eRE_M$, which is the classical maximum energy an electron can acquire in the laser field. For $N \ll \delta = 2\Omega_R/\omega$ the intensity of the Nth harmonic from asymptotic properties of $J_N(\delta)$ is given by

$$I_N \propto \omega_0^2/(\omega\Omega_R). \qquad (13)$$

Clearly, the harmonic intensity decreases for high laser intensities, approaching the zero efficiency of degenerate states. In fact, one sees from Eq. (10) that $x(t)$ is vanishing for zero energy separation of a two-level system, i.e., $\omega_0 = 0$. Furthermore, from Eq. (4) it can be shown that the acceleration $\ddot{x}(t)$, which enters Maxwell's equation as the source term for HG [18], is *exactly* zero for degenerate two-level systems. This therefore justifies our claim at the beginning of this section that degenerate atomic transitions, e.g., $ns \rightarrow np$, do not contribute to HG in atoms but do so in molecules where they are no longer degenerate. Furthermore, the lowest CR transition, $1\sigma_g \rightarrow 1\sigma_u$ in Fig. 1, which is isolated from other transitions at large R, should exactly satisfy the strong coupling criteria, $\delta = 2\Omega_R/\omega \gg 1$. We next turn to

examine these asymptotic results by numerical experiments.

III. NUMERICAL METHODS

The H_2^+ molecular ion consists of two protons at an internuclear distance R with a single electron bound to the nuclei. An exact quantum description of H_2^+ in a strong laser field is difficult to obtain. As a first approximation we regard the H_2^+ system as a single electron quantum system in the Coulomb potential of the two motionless protons (adiabatic approximation) with the internuclear separation R varying as a parameter to represent various initial vibrational excitations. If the external laser field is chosen to be a classical, linearly polarized field along the internuclear axis, the H_2^+ problem reduces to solving a three-dimensional (3D) time-dependent Schrödinger equation. A numerical scheme which takes advantage of the cylindrical symmetry of the problem by using a Bessel-Fourier expansion and the efficiency of the FFT (fast Fourier transform) dependent split-operator technique was proposed by us to calculate ionization rate of the H_2^+ in a laser field [21]. The same computer code is used in the present work to obtain the time-dependent wave function. We therefore do not repeat the details of solving the 3D Schrödinger equation and refer the readers to the details in Ref. [21].

Some aspects of calculation of the HG power spectra using the time-dependent wave function, however, deserve to be commented on. One is that the HG spectra can be calculated by performing a Fourier transformation of either the time-dependent dipole moment (in atomic units)

$$d(t) = \langle\psi(t)|z|\psi(t)\rangle, \qquad (14)$$

or the time-dependent electron acceleration (in atomic units), the latter being the source term for HG in Maxwell's equations,

$$a(t) = \frac{d^2}{dt^2}\langle\psi(t)|z|\psi(t)\rangle. \qquad (15)$$

Here $\psi(t)$ denotes the exact time-dependent wave function and z is the coordinate along the direction of laser polarization. There have been a number of discussions on this issue [22–24]. Our experience is that provided an ω^4 factor is taken into account the two schemes are generally in good agreement with the exception that the acceleration scheme usually produces much lower background in the spectra than the dipole moment scheme (the ω^4 factor is necessary in order to take into account the phase volume of the spontaneously emitted radiation frequencies). As a consequence of the difference of the background, some high harmonic peaks are immersed into the background in the dipole moment scheme. Figure 2 shows a clear example of this. Nevertheless, for most purposes of our present study, such as the examination of the "cutoff" of the plateau, the dipole moment scheme is often found to be adequate.
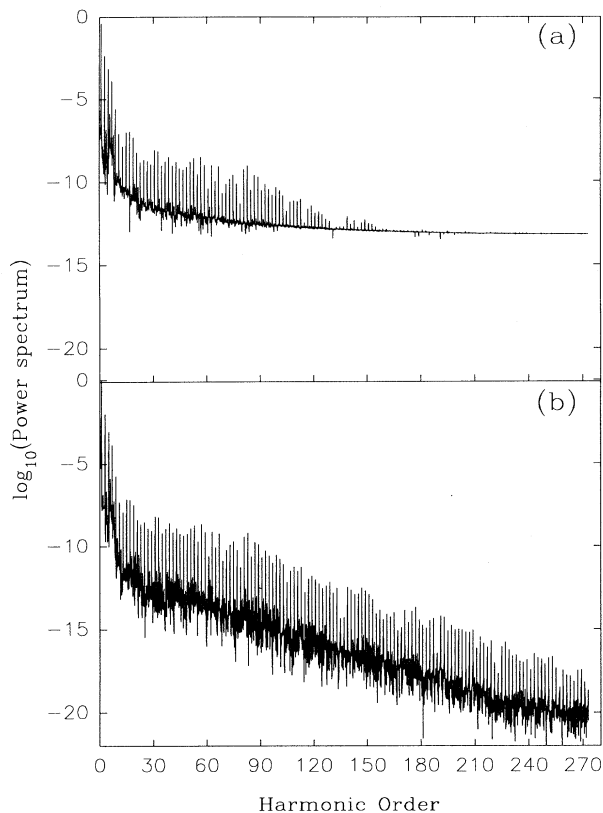
FIG. 2. Harmonic-generation spectra of H_2^+ at $R = 3$ a.u., $I = 2.42 \times 10^{14}$ W/cm^2, $\lambda = 1064$ nm. (a) Spectrum calculated using the dipole scheme; (b) spectrum calculated using the acceleration scheme.

In all our calculations the laser turns on linearly for around five cycles and is then kept constant. The power spectra are usually calculated by Fourier transforming the dipole moment or acceleration between 11 and 26 cycles. The several cycle "waiting" is very useful to reduce the background of the spectra as it allows the transient states induced by the turn on of the laser pulse to decay [4,25].

IV. RESULTS AND DISCUSSIONS

The H_2^+ molecular ion is the simplest molecule representing the one electron bond. The electronic energy levels of H_2^+ vary with the internuclear distance R from the He$^+$ limit (small R) to the H atom limit (large R). The ionization potential varies from 2 a.u. to 0.5 a.u. accordingly (see Fig. 1). The lowest two energy levels, the ground $1\sigma_g$ state and the antibonding $1\sigma_u$ state, which are well separated at the He$^+$ limit, approach each other at the H atom limit forming a pair of CR states which are very strongly coupled to electromagnetic fields at large R [6,7]. It is of interest to see whether this strong coupling aspect of the CR transitions plays any role in harmonic generation.

We begin by comparing Figs. 3 and 2, the first for H_2^+ at the equilibrium distance, $R = 2$ a.u., whereas $R = 3$ a.u. corresponds to a stretched ion, Fig. 2. From both figures one sees a plateau in the intensity of the harmonics generated, with a clear cutoff. Thus for $R = 2$ and 3 a.u., $\lambda = 1064$ nm, the cutoff occurs at $N_m = 155$ and 83 for intensities 4.24×10^{14} and 2.42×10^{14} W/cm^2, respectively. This is to be compared to the values of the theoretical cutoff tabulated in Table I according to the two-level formula, Eq. (12), or the ionizing electron formula [4,5]:

$$N_m = (I_p + 3.17U_p)/\hbar\omega. \qquad (16)$$

Here I_p is the ionization potential (see Table I) and U_p denotes the ponderomotive energy $U_p = e^2E_m^2/4m\omega^2$. The $3.17U_p$ contribution can be explained by classical arguments. For example, Corkum has shown that in a linearly polarized laser field, the maximum kinetic energy of an electron passing through the nucleus is $3.17U_p$ [5]. Equation (16) is a useful formula which gives a reasonable estimation of the atomic, i.e., the longest "plateau." This formula is usually valid for the cases where this plateau is well established, i.e., $I_p + 3.17U_p$ is many times of the photon energy. Table I indeed shows that it applies to the atomic plateau. As calculated in Table I, both Figs. 2 and 3 show intensity cutoffs at values of N_m respecting very well formula (16). Of note is that Fig. 2, which represents the stretched molecule, exhibits harmonic-generation efficiencies of at least two orders of magnitude greater than that of Fig. 3, the equilibrium configuration. This is even more remarkable since the stretched molecule is at lower intensity (2.42×10^{14} W/cm^2) but nevertheless undergoes twice as much ionization as the equilibrium configuration which is at higher intensity (4.24×10^{14} W/cm^2), see Table I. We have noted previously that H_2^+ ionization rates increase for the stretched configuration, approaching that of the H atom at large distances. For He$^+$, the united atom ($R = 0$) limit, an
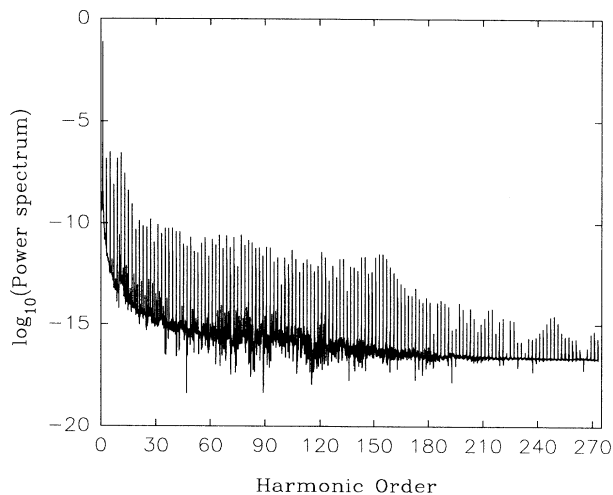

FIG. 3. Harmonic-generation spectrum of H_2^+ at $R = 2$ a.u., $I = 4.24 \times 10^{14}$ W/cm^2, $\lambda = 1064$ nm.

TABLE I. A comparison of the cutoff of the harmonic order N_m. I_p—ionization potential; U_p—ponderomotive potential.

I (10^{14} W/cm^2)	λ (nm)	N_m [a]	N_m [b]	N_m [c]	R (a.u.)	I_p (a.u.)	R_I (s^{-1}) [d]
65	228	28.4		27	0 [e]	2.0	5.8×10^{12}
4	228	6.6	1.1	5	2	1.1	9.0×10^{12}
2	228	5.1	1.1	f	3	0.91	6.0×10^{13}
1	228	2.8	1.6	f	6	0.68	1.5×10^{13}
1	228	2.8		f	∞ [g]	0.5	6.0×10^{13}
40	1064	1202			0 [e]	2.0	9.0×10^{10}
4.24	1064	148	5.0	155	2	1.1	1.0×10^{11}
2.42	1064	91	5.8	83	3	0.91	2.5×10^{11}
0.259	1064	23	3.8	f	6	0.68	4.0×10^{9}
0.579	1380	56	8.6	7	7	0.65	1.6×10^{12}
1	1380	83	11.3	15	7	0.65	9.0×10^{12}
0.579	1380	55	12.3	13	10	0.60	5.0×10^{11}
1	1380	81	16.1	15(85)	10	0.60	1.0×10^{13}
0.4	1064	23		23	∞ [g]	0.5	1.5×10^{10}
0.579	1380	52		69	∞ [g]	0.5	3.0×10^{10}
1	1380	78		85	∞ [g]	0.5	1.5×10^{12}

[a] $I_p + 3.17U_p$ formula.
[b] Two-level formula $2\Omega_R/\omega$.
[c] The present work for $H_2{}^+$.
[d] R_I—ionization rate.
[e] He^+ limit.
[f] There are too few peaks to determine the plateau or the cutoff.
[g] H atom limit.

ionization rate of 9×10^{10} s^{-1}, is obtained at an intensity of 4×10^{15} W/cm^2 (see Table I) and wavelength 1064 nm. For the latter, the harmonic-generation efficiencies were found to be two orders of magnitude lower than the equilibrium $H_2{}^+$ for the same wavelength excitation. We conclude therefore that in $H_2{}^+$ the harmonic-generation efficiency improves with increasing internuclear distance at 1064-nm-long-wavelength excitation.

At short-wavelength excitation $\lambda = 228$ nm, one finds that $H_2{}^+$ at $R = 6$ a.u., Fig. 4, gives a HG spectrum nearly identical to the H atom, Fig. 5, at the same in-
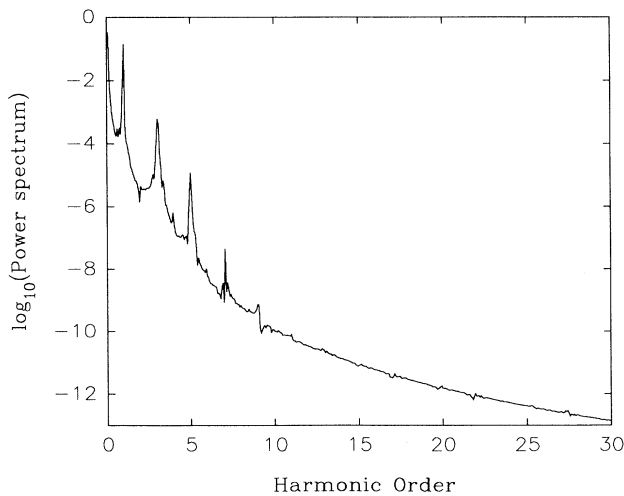

FIG. 4. Harmonic-generation spectrum of $H_2{}^+$ at $R = 6$ a.u., $I = 1 \times 10^{14}$ W/cm^2, $\lambda = 228$ nm.
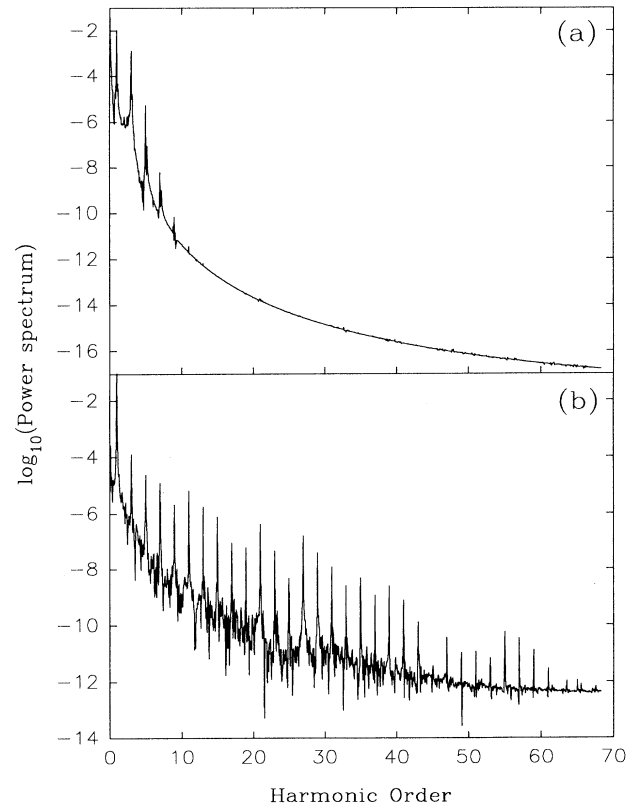

FIG. 5. Harmonic-generation spectra of H atom and He^+: (a) H atom at $I = 1 \times 10^{14}$ W/cm^2, $\lambda = 228$ nm; (b) He^+ at $I = 6.5 \times 10^{15}$ W/cm^2, $\lambda = 228$ nm.

tensity, i.e., 10^{14} W/cm^2 (we include also He$^+$ showing that one must go to much higher intensities to obtain comparable HG efficiencies). No cutoff is observable due to the high photon frequency. For the same conditions of intensity and wavelength, H$_2$ $^+$ at $R = 3$ a.u. shows similar HG efficiencies as Figs. 4 and 5, the only difference being that the $R = 3$ a.u. molecular ion exhibits Rabi splittings of the harmonics. This is due to the fact that in the stretched configuration, at $\lambda = 228$ nm the single photon absorption from the $1\sigma_g$ to $1\sigma_u$ state is now resonant, hence causing laser-induced avoided crossings [11,12] and Rabi splittings [26]. We conclude therefore that for high frequency excitation H$_2$ $^+$ and H behave in similar fashion with respect to HG.

Manifestation of isolated two-level effects, i.e., the $1\sigma_g \rightarrow 1\sigma_u$ transition, are clearly visible in Fig. 6 for H$_2$ $^+$ at $R = 6$ a.u. and $\lambda = 1064$ nm excitation. This is confirmed by Fig. 7, which is an exact two-level calculation of HG for the same conditions as H$_2$ $^+$, i.e., the energy separation $\omega_0 = E_{1\sigma_g} - E_{1\sigma_u} = 0.52$ eV at $R = 6$ a.u. (Fig. 1), $\Omega_R = eRE_M/2$ with $I = 2.59 \times 10^{13}$ W/cm$^2 = cE_M^2/8\pi$. Using Eq. (7), this gives $\Omega_R = 2$ eV for the conditions for Figs. 6 and 7. Clearly $\Omega_R/\omega_0 > 1$, so that we are in the strong coupling regime for which the two-level model was solved in Sec. II. We note that the H$_2$ $^+$ and two-level HG spectra agree extremely well. The relative intensities of $N = 1, 3, 5$, and 7 harmonic are comparable for both spectra. Furthermore, in both cases *even* harmonics appear and are split in two, with the same energy splitting. The latter effect is due to the large Rabi splittings [26,27] of the odd harmonics so that these split lines appear to converge towards even harmonics. Alternatively, one can show that there exist quasienergy (Floquet or dressed) states whose energy separation is given by the following relation [3,28,29]:

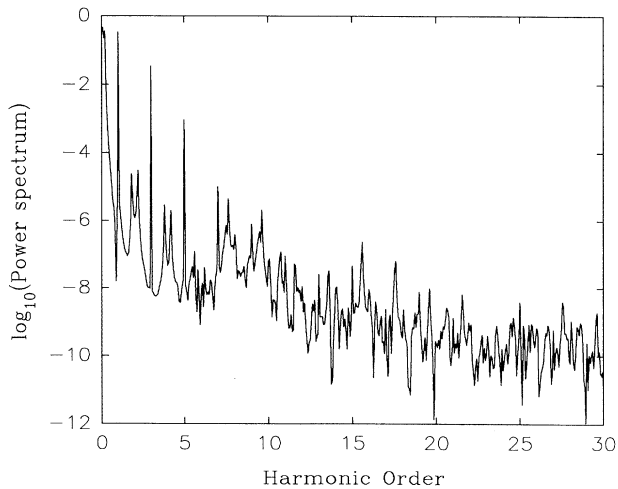$$\omega_q = \omega_0 J_0(2\Omega_R/\omega), \qquad (17)$$

FIG. 6. Harmonic-generation spectrum of H$_2$ $^+$ at $R = 6$ a.u., $I = 2.59 \times 10^{13}$ W/cm^2, $\lambda = 1064$ nm.
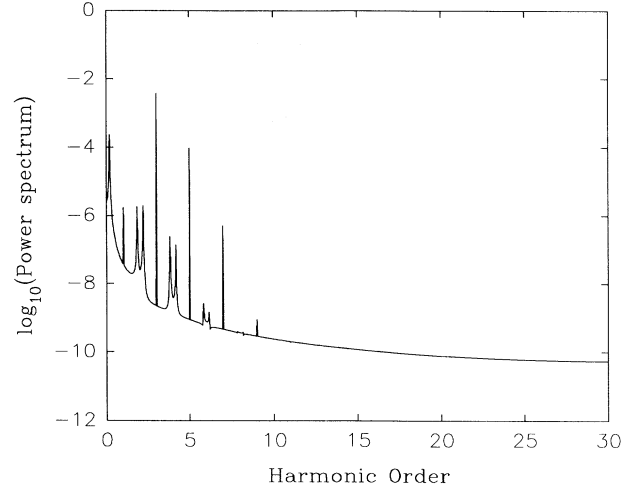

FIG. 7. Same as Fig. 6 but exact two-level model calculation.

where, as in Sec. II, ω_0 is the unperturbed $1\sigma_g - 1\sigma_u$ energy separation, J_0 is the zeroth-order Bessel function, Ω_R is the Rabi frequency, and ω is the photon frequency. It can be shown that each harmonic will appear at the frequencies [3]

$$\omega_{\rm HG} = 2n\omega \pm \omega_q. \qquad (18)$$

Inserting the appropriate values of ω_0, Ω_R, and ω for Figs. 6 and 7 into Eq. (17) reproduces the even harmonic doublets exactly. Thus Figs. 6 and 7 illustrate the dominant effect of the isolated $1\sigma_g \rightarrow 1\sigma_u$ transition on HG of H$_2$ $^+$ at $R = 6$. Comparison with HG efficiencies from the H atom under identical conditions shows that H$_2$ $^+$ at $R = 6$ a.u. generates low harmonics at efficiencies two orders of magnitude larger than for H. The quasi-two-level structure has also been confirmed in our calculations by projecting the time-dependent wave function onto the field-free ground state. The ground state has been found to populate and depopulate during the laser pulse in agreement with the Rabi oscillation in a two-level system [18].

Finally, in order to verify the properties of the two-level system as derived in Sec. II, we compare in Fig. 8 the HG spectra for H$_2$ $^+$ at $R = 10$ a.u., $I = 10^{14}$ W/cm^2, $\lambda = 1380$ nm with the equivalent two-level model, Fig. 9, and the H atom ($R = \infty$, Table I), under the same laser excitation conditions, Fig. 10. In the H$_2$ $^+$ case, Fig. 8, a first low frequency plateau between $N = 1$ and 15 is clearly discernible and correlates extremely well with the two-level plateau, Fig. 9, although the molecular HG efficiency is much larger than the two-level efficiency. This is accompanied by even harmonics in both cases, which correspond to zero energy separation (zeroth of J_0) in Eq. (18) of the dressed states. One can therefore associate this low energy plateau with the isolated $1\sigma_g \rightarrow 1\sigma_u$ transition. Such a low frequency plateau is not easily identifiable in H, Fig. 10. We emphasize further that the
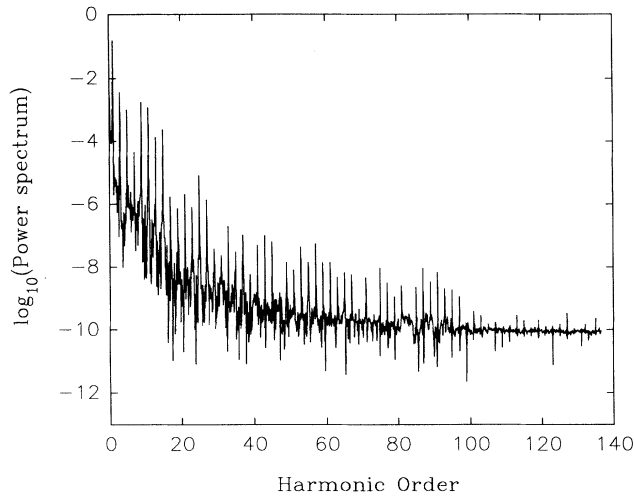
FIG. 8. Harmonic-generation spectrum of H_2^+ at $R = 10$ a.u., $I = 1.0 \times 10^{14}$ W/cm^2, $\lambda = 1380$ nm.
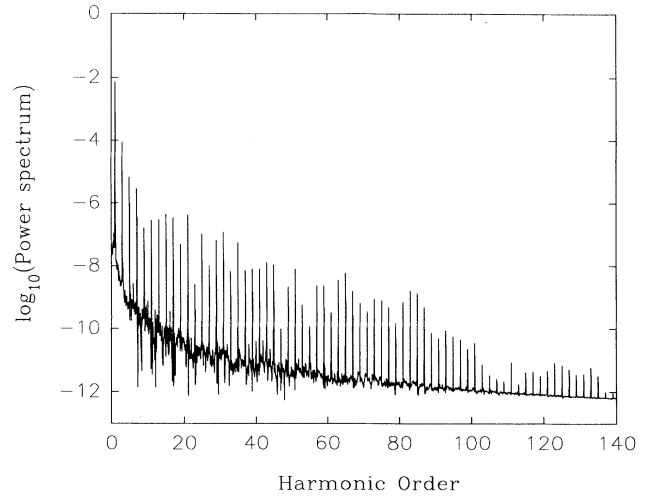

FIG. 10. Harmonic-generation spectrum of H atom at $I = 1.0 \times 10^{14}$ W/cm^2, $\lambda = 1380$ nm.

low frequency plateau in H_2^+ exhibits HG efficiencies of about 10^3 larger than in H under the same conditions, even though the ionization rate is ten times larger in H_2^+ than H (Table I). Table I summarizes the cutoffs N_m for the HG plateaus as calculated from the two-level model, Eq. (12), and the ionization electron model, Eq. (16). Thus Figs. 8 and 9 agree with $N_m = 15$ and also with Table I for the low frequency plateau. This is attributed to molecular CR transitions, in particular the $1\sigma_g \rightarrow 1\sigma_u$ transition which is well isolated (Fig. 1). A high frequency plateau cutoff appears in both Figs. 8 and 10 at about the same value of $N_m \approx 85$ (there is a slight ionization potential difference I_p whereas U_p should be the same in both the molecular ion and the atom). This high frequency plateau with identical cutoff in both H_2^+ and H can be clearly identified as of atomic character.
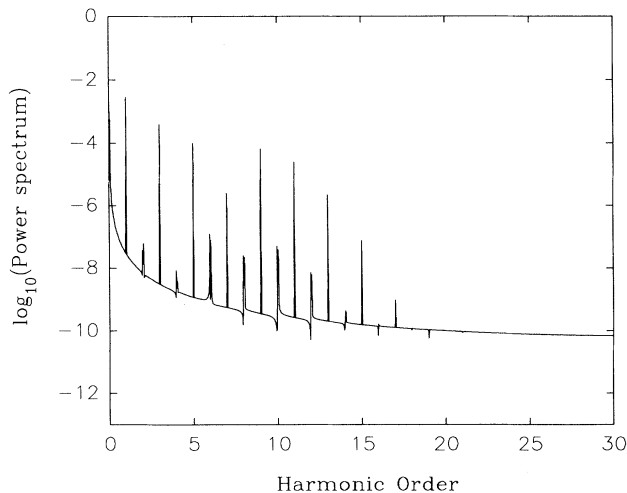

FIG. 9. Same as Fig. 8 but exact two-level model calculation.

We also note that the HG efficiencies of the second high frequency plateau are about the same in both cases.

V. CONCLUSIONS

In comparing HG from H_2^+ with respect to the separated atom H ($R = \infty$) or the united atom, He$^+$ ($R = 0$), we have emphasized that degenerate atomic transitions emit no harmonics (Sec. II). In the molecular ion, these degenerate atomic transitions become nondegenerate (see Fig. 1) and will contribute now to HG. Furthermore, new transitions, between charge-resonance states, produce transition moments which diverge as $R/2$. These CR transitions couple very strongly to the electromagnetic field at large distance and give rise to a low frequency HG plateau in H_2^+ with very high efficiency, exceeding atomic HG efficiencies by about three orders of magnitude. The signature of this low energy plateau is its similarity to the HG spectra of two-level systems. High energy plateaus remain and can be attributed to atomiclike excitations in the molecular ion, albeit the molecular HG efficiencies are usually almost two orders of magnitude larger than H at the same intensities due to the presence of new (nondegenerate vs degenerate) transitions and the CR states.

Both cutoff formulas, Eq. (12) for large R and Eq. (16) are generally well respected in H_2^+ (see Table I). It is to be emphasized that the high energy (atomic) cutoff, Eq. (16), is derived from considerations of the maximum kinetic energy attainable by an ionizing electron [5]. Equation (12) can be rationalized on the same basis, i.e., $2\Omega_R = eRE_M$ is the maximum energy acquired by an electron in moving from proton A to B in H_2^+ in the presence of the field E_M. Thus both plateau cutoffs obey the predictions of a simple classical model. The distinctive feature of the H_2^+ HG spectra is the existence of two plateaus with different cutoffs, Eqs. (12) and (16). We

are currently investigating the possibilities of extending the low energy CR state plateau to overlap with the high energy atomiclike plateau by examining electrons in polyatomic centers, the interest being that CR transitions produce much more efficient HG. A further advantage of molecular ions over atoms is the variable ionization potentials as a function of internuclear distance. Since in this work the fixed nuclei approximation is used, the results need to be integrated over the size of the molecular vibrational wave packet (its size is typically the width of the ground state wave function of H_2 or $H_2{}^+$) in a more realistic situation. The system therefore behaves as an ensemble of the "frozen" molecular ions in various ionization potentials. One may expect the molecular ions to exhibit wider "windows" for efficient HG than pure atomic system due to the strong dependence of the HG on the ionization potential. Alternatively one can imagine stretching the molecular ion by a delayed two pulse sequence, i.e., dissociation first followed by HG by the second delayed pulse. This would help enhance HG efficiencies due to the importance of CR transitions at large R. Dynamics of $H_2{}^+$ photodissociation in a two-potential approximation ($1\sigma_g - 1\sigma_u$) have been recently investigated by [30] and [11] and stabilization has been again confirmed. Further calculations by Aubanel and Bandrauk [31] have shown that one can obtain rapid high level inversion by a pump-dump scheme using the continuum as the intermediate state. This calculation shows a way to prepare $H_2{}^+$ with large internuclear distances efficiently.

ACKNOWLEDGMENTS

[1] A. L'Huillier, K. J. Schafer, and K. C. Kulander, J. Phys. B **24**, 3315 (1991).
[2] J. L. Krause, K. J. Schafer, and K. C. Kulander, Chem. Phys. Lett. **178**, 573 (1991).
[3] M. Yu. Ivanov, P. B. Corkum, and P. Dietrich, Laser Phys. **3**, 375 (1993).
[4] J. L. Krause, K. J. Schafer, and K. C. Kulander, Phys. Rev. A **45**, 4998 (1992); Phys. Rev. Lett. **68**, 3535 (1992).
[5] P. B. Corkum (unpublished).
[6] R. S. Mulliken, J. Chem. Phys. **7**, 20 (1939).
[7] A. D. Bandrauk and M. L. Sink, Chem. Phys. Lett. **57**, 569 (1978); J. Chem. Phys. **74**, 1110 (1981).
[8] A. D. Bandrauk and J. F. McCann, Comments At. Mol. Phys. **22**, 325 (1989); Phys. Rev. A **42**, 2806 (1990).
[9] A. D. Bandrauk and J. M. Gauthier, J. Opt. Soc. Am. B **7**, 1420 (1990).
[10] A. D. Bandrauk, E Contant, and J. M. Gauthier, J. Phys. (France) I **1**, 1033 (1991).
[11] E. Aubanel, P. Rancourt, and A. D. Bandrauk, Chem. Phys. Lett. **197**, 419 (1992).
[12] E. Aubanel, J. M. Gauthier, and A. D. Bandrauk, Phys. Rev. A (to be published).
[13] J. W. Verschuur, L. D. Noordam, and H. B. van Linden, Phys. Rev. A **40**, 4383 (1989).
[14] P. H. Bucksbaum, A. Zavriyev, H. G. Muller, and D. W. Schumacher, Phys. Rev. Lett. **64**, 1883 (1990).
[15] S. Allendorf and A. Szöke, Phys. Rev. A **44**, 578 (1991).
[16] M. Yu. Ivanov and P. B. Corkum, Phys. Rev. A **48**, 580 (1993).
[17] J. C. Slater, *Quantum Theory of Molecules and Solids* (McGraw-Hill, New York, 1963), Vol. 1.
[18] L. Allen and J. H. Eberly, *Optical Resonance and Two-Level Atoms* (Wiley Interscience, New York, 1975).
[19] *Handbook of Mathematical Functions*, edited by M. Abramowitz and I. A. Stegun (Dover, New York, 1972).
[20] S. Chelkowski and A. D. Bandrauk (unpublished).
[21] S. Chelkowski, T. Zuo, and A. D. Bandrauk, Phys. Rev. A **46**, 5342 (1992).
[22] B. Sundaram and P. W. Milonni, Phys. Rev. A **41**, 6571 (1990).
[23] K. Burnett, V. C. Reed, J. Cooper, and P. L. Knight, Phys. Rev. A **45**, 3347 (1992).
[24] K. LaGattuta, J. Mod. Opt. **39**, 1181 (1992).
[25] S. Chelkowski and A. D. Bandrauk, Phys. Rev. A **44**, 788 (1991).
[26] B. R. Mollow, Phys. Rev. **188**, 1969 (1969).
[27] C. Cohen-Tannoudji, J. Dupont-Roc, and G. Grynberg, *Atom-Photon Interactions* (Wiley, New York, 1992).
[28] A. G. Fainshtein, N. L. Manakov, and L.-P. Rapoport, J. Phys. B **11**, 2561 (1978).
[29] J. M. Gomez Llorente and J. Plata, Phys. Rev. A **45**, 6958 (1992).
[30] G. Yao and S. Chu, Chem. Phys. Lett. **197**, 413 (1992).
[31] E. Aubanel and A. D. Bandrauk, J. Phys. Chem. (to be published).